Overcoming thickened pathological skin in psoriasis via iontophoresis combined with tight junction-opening peptide AT1002 for intradermal delivery of NF-κB decoy oligodeoxynucleotide

Tatsuya Fukuta,[1,#] Daichi Tanaka,[1,#], Shinya Inoue, Kohki Michiue, Kentaro Kogure[1, *]

[1]*Department of Pharmaceutical Health Chemistry, Graduate School of Biomedical Sciences, Tokushima University, Shomachi 1, Tokushima 770-8505, Japan*

[*]Corresponding author: Kentaro Kogure

TEL: +81-88-633-7248

FAX: +81-88-633-9572

Email: kogure@tokushima-u.ac.jp

Department of Pharmaceutical Health Chemistry, Graduate School of Biomedical Sciences, Tokushima University, Shomachi 1, Tokushima 770-8505, Japan

[#]These authors contributed equally to this work

Abstract

Transdermal delivery of nucleic acid therapeutics has been demonstrated to be effective for psoriasis treatment. We previously reported the utility of iontophoresis (IP) using weak electric current (0.3-0.5 mA/cm^2) for intradermal delivery of nucleic acid therapeutics via weak electricity-mediated intercellular junction cleavage, and subsequent exertion of nucleic acid function. However, the thickened pathological skin in psoriasis hampers permeation of IP-administered macromolecules. Thus, approaches are needed to more strongly cleave intercellular spaces and overcome the psoriatic skin barrier. Herein, we applied a combination of tight junction-opening peptide AT1002 with IP, as synergistic effects of weak electricity-mediated intercellular junction cleavage and the tight junction-opening ability of AT1002 may help overcome thickened psoriatic skin and facilitate macromolecule delivery. Pretreatment with IP of an AT1002 analog exhibiting positively-charged moieties before fluorescence-labeled oligodeoxynucleotide IP resulted in the oligodeoxynucleotide permeation into psoriatic skin, whereas IP of the oligodeoxynucleotide alone did not. Moreover, psoriasis-induced upregulation of inflammatory cytokine mRNA levels was significantly suppressed by NF-κB decoy oligodeoxynucleotide IP combined with the AT1002 analog, resulting in amelioration of epidermis hyperplasia. These results suggest that synergistic effects of IP and an AT1002 analog can overcome thickened psoriatic skin and enable intradermal delivery of NF-κB decoy oligodeoxynucleotide for psoriasis treatment.

Keywords

Transdermal drug delivery; Iontophoresis; Nucleic acid therapeutics; NF-κB decoy oligodeoxynucleotide; AT1002; Psoriasis

1. **Introduction**

Psoriasis is an immune-mediated disease that causes chronic skin inflammation and affects approximately 2–3% of the general population worldwide (Goldminz et al., 2013). Hyperproliferation and aberrant differentiation of keratinocytes is reported to be induced in psoriasis by dysregulated immune response, and proliferating keratinocytes secrete several cytokines to migrate immune cells including T cells and leukocytes into epidermis and dermis layers of inflamed psoriatic skin (Hawkes et al., 2017). These abnormal inflammatory reactions cause epidermis hyperplasia, the most distinctive histological changes in psoriasis that differ from other inflammatory skin diseases (Tonel and Conrad, 2009). Although the pathogenesis of psoriasis is not fully understood, systemic treatment with anti-tumor necrosis factor-α (TNF-α) monoclonal antibody and anti-interleukin-17A (IL-17A) antibody has been clinically proven to inhibit immune responses and the pathological progression of psoriasis. Treatment of psoriasis with such antibody drugs is reported to be effective via modulation of the nuclear factor-κB (NF-κB) signaling pathway, a main regulator of immune responses (Veilleux and Shear, 2017). However, systemic administration of these drugs may be associated with adverse side effects, so that development of therapeutic approaches via topical routes, with minimal side effects, is required.

Transdermal delivery of nucleic acid therapeutics, such as small interfering RNA (siRNA) and nuclear factor-κB (NF-κB) decoy oligodeoxynucleotide (ODN), is a promising strategy for treatment of skin diseases, such as atopic dermatitis and psoriasis (Hashim et al., 2010; Mandal et al., 2020). Compared with invasive administration methods using needles, topical delivery is a non-invasive and patient-compliant method, and is therefore attracting considerable attention as a new administration route of nucleic acids with a favorable safety profile (Anselmo et al., 2019). While hydrophobic drugs with low molecular weights are generally suitable for transdermal delivery, delivery of nucleic acid therapeutics has typically been challenging owing to their high molecular weights and the presence of rigid skin barriers (Prausnitz and Langer, 2008). Recently, however, several technologies, including electroporation (Banga and Prausnitz, 1998), microneedles (Mikszta

et al., 2002), ionic liquid (Dharamdasani et al., 2020), and iontophoresis (IP) (Hashim et al., 2010), have been reported to enable successful delivery of nucleic acids into the skin. These approaches have also been applied for transdermal delivery of other macromolecular drugs, including proteins and nucleic acid therapeutics (Anselmo et al., 2019).

Among transdermal technologies described above, we demonstrated the utility of the IP using a weak electric current (0.3–0.5 mA/cm^2). This system is non-invasive and does not require the use of needles (Hasan et al., 2020). IP has mostly been applied for transdermal delivery of hydrophobic and charged low-molecular weight drugs, such as lidocaine and dexamethasone, via electroosmosis and electrorepulsion (Guy et al., 2000; Lark and Gangarosa Sr, 1990; Spierings et al., 2008). However, we succeeded in the intradermal delivery of several hydrophilic macromolecules, such as nucleic acid therapeutics (siRNA and CpG oligo DNA) (Kigasawa et al., 2010; Kigasawa et al., 2011), antibodies (Fukuta et al., 2020), and charged nanoparticles (liposomes and nanogels) (Kajimoto et al., 2011; Toyoda et al., 2015), and demonstrated the subsequent exertion of their respective functions *in vivo*. In particular, we demonstrated efficient silencing of target mRNA by iontophoretic delivery of siRNA into the skin of atopic dermatitis model rats (Kigasawa et al., 2010). Results of another study from our laboratory provided insights into the mechanism of IP-mediated permeation of macromolecules into the skin. In particular, Ca^{2+} influx into skin cells and subsequent intracellular signal activation are induced via IP, which leads to a decrease in expression of gap junction protein connexin 43 and depolymerization of tight junction-associated polymerized actin, resulting in cleavage of intercellular junctions (Hama et al., 2014). Moreover, treatment with weak electric current can induce cellular uptake of siRNA via a unique endocytosis process, in which endosomes are formed that can leak substances with molecular weights <70,000 that were taken up by cells; these findings explain how siRNA reaches the cytoplasm of IP-treated skin tissue (Hasan et al., 2016a; Hasan et al., 2016b; Torao et al., 2020). Based on these findings, if nucleic acid therapeutics (e.g., NF-κB decoy ODN and siRNA) can successfully be intradermally delivered into psoriatic skin via IP, it is expected that transdermal delivery of nucleic acid therapeutics by IP could

be applied for the treatment of not only atopic dermatitis but also other inflammatory skin diseases including psoriasis. However, we recently found that antibodies (Fukuta et al., 2020) and fluorescence-labeled ODN (data are shown in Results section) delivered by IP were unable to permeate the thickened pathological skin associated with psoriasis conditions. As a result of this finding, in our previous reports on psoriasis treatment by IP of an anti-tumor necrosis factor (TNF)-α antibody, multiple doses were needed to obtain therapeutic effects, whereas a single dose hardly ameliorated psoriasis. These results were suggested to be due to formation of a thickened skin barrier caused by epidermis hyperplasia, a distinct symptom of psoriasis, which is caused by excessively aberrant keratinocyte differentiation and immune cell migration in psoriatic skin (Lowes et al., 2007). Hence, to overcome the thickened pathological skin barrier and achieve efficient treatment of psoriasis, approaches are needed, in addition to IP, to more strongly cleave the intercellular spaces.

To achieve efficient delivery of macromolecular drugs into psoriatic skin through transdermal route, we focused on the functional peptide AT1002, which was reported to exhibit tight junction-opening abilities (Goldblum et al., 2011). AT1002 is a synthetic six-mer peptide (Phe-Cys-Ile-Gly-Arg-Leu) identified from structure-activity relationship studies of Zonula occuluta toxin (Zot), which can reversibly open tight junctions (Watts et al., 2005). AT1002 retains the tight junction-opening ability of Zot without the associated toxicity, and can decrease the expression of tight junction proteins resulting in promotion of paracellular transport of combined administered drugs across the epithelial barrier in nasal mucosa and intestine (Song et al., 2008a, b). Uchida et al. reported that topical application of AT1002 to tape-striped mouse dorsal skin that lacks a skin barrier stratum corneum (SC) reversibly reduced ZO-1 expression, which led to increased intradermal delivery efficiency of siRNA into the healthy skin without SC (Uchida et al., 2011b). Uchida et al. also demonstrated that topically applied siRNA combined with AT1002 and a cell penetrating peptide to promote cellular uptake of siRNA could suppress target mRNA expression and ameliorate apoptotic symptoms (increase in ear thickness) in the ear skin of atopic dermatitis model mice (Uchida et al., 2011a). These findings highlight the usefulness of the tight junction-opening peptide

AT1002 for intradermal delivery of siRNA. However, it was reported that under psoriatic conditions, anomalous tight junctions are present in thickened pathological epidermis by broad localization of tight junction proteins, including ZO-1 from the stratum spinosum to the stratum granulosum (Kirschner et al., 2009). Therefore, if AT1002 can be transdermally delivered into broader and deeper regions of the inflamed thickened skin (i.e., relative to topical application), AT1002 is expected to regulate the anomalous tight junctions in psoriatic skin via reduction of ZO-1 expression, thus overcoming the thickened psoriatic skin barrier for transdermal delivery of nucleic acid therapeutics.

Considering the above findings, we hypothesized that combination of IP and AT1002 may overcome the abnormal skin barrier under psoriatic conditions. Combination of IP and AT1002 may result in AT1002 being intradermally delivered into deep regions of psoriatic skin to allow for synergistic effects of the tight junction-opening ability of AT1002 and intercellular junction cleavage via weak electricity to promote intradermal permeation of IP-administered nucleic acid therapeutics. However, the intradermally delivered nucleic acid therapeutics (e.g. NF-κB decoy ODN and siRNA) must be taken up by skin cells and reach the cytoplasm to exert their functions. Thus, another advantage of the combination of IP and AT1002 is that since IP induces cellular uptake of macromolecular drugs via unique endocytosis, and resultant endosomes can leak macromolecules with molecular weight <70,000, the intradermally permeated nucleic acid therapeutics may be efficiently taken up by inflamed skin cells. To prove this hypothesis, we herein used NF-κB decoy ODN as a representative nucleic acid therapeutic and applied the combination system of IP and AT1002 in psoriasis model rats. NF-κB is a key regulatory element in various inflammatory pathways, and is known to be a crucial mediator involved in pathological progression of psoriasis, which causes chronic inflammatory symptoms in the skin (Goldminz et al., 2013). Psoriatic inflammation is induced by marked activation of NF-κB pathways, followed by excess production of inflammatory cytokines, such as TNF-α, IL-1, IL-6, IL-17, etc. Hence, selective inhibition of NF-κB signaling by intradermal delivery of NF-κB decoy ODN is considered a promising approach to treat psoriasis (Gilmore and Garbati, 2010; Isomura and Morita, 2006).

In the present study, we first examined intradermal delivery of fluorescence-labeled NF-κB decoy ODN via IP alone and evaluated the effect of combination with AT1002 on its distribution in the inflamed skin of psoriasis model rats. We investigated the function of NF-κB decoy ODN delivered via combination of IP and AT1002 in the model rats, and also evaluated the therapeutic effects on psoriasis.

2. Material and Methods

2.1. Reagents

NF-κB decoy oligodeoxynucleotide (ODN) and 6-carboxyfluorescein (FAM)-labeled NF-κB decoy ODN (FAM-ODN; FAM labeling at the 3' end) were synthesized by Eurofins Genomics (Tokyo, Japan). The sequences of the NF-κB decoy ODN were as follows: 5'-CCTTGAAGGGATTTCCCTCC-3' and 5'-GGAACTTCCCTAAAGGGAGG-3'. The AT1002 analog (Arg-Arg-Arg-Gly-Gly-Phe-Cys-Ile-Gly-Arg-Leu) and the control 10-mer peptide having three Arg and two Gly without the sequences of AT1002 (Arg-Arg-Arg-Gly-Gly-Leu-Gly-Cys-Arg-Phe-Ile) were synthesized by Peptide Institute, Inc. (Osaka, Japan). Fluorescein isothiocyanate (FITC)-labeled AT1002 analog (FITC-ε-aminocaproic acid-Arg-Arg-Arg-Gly-Gly-Phe-Cys-Ile-Gly-Arg-Leu) was also synthesized by Peptide Institute, Inc. Beselna cream 5%® was purchased from Mochida Pharmaceuticals (Tokyo, Japan). OCT compound, Perma Fluor Aqueous Mounting Medium, and Entellan New® (hydrophobic mounting medium) were obtained from Sakura Finetek (Tokyo, Japan), Thermo Fisher Scientific (Tokyo, Japan), and Merck Millipore (Tokyo, Japan), respectively. Isoflurane, Mayer's hematoxylin solution and 1% eosin Y solution were purchased from FujiFilm Wako Pure Chemical (Osaka, Japan). QIAzol Lysis reagent and RNeasy Plus Universal Midi Kit were obtained from QIAGEN (Hilden, Germany). PrimeScript RT Master Mix (Perfect Real Time) and TB Green™ Premix Ex Taq™ II (Tli RNaseH Plus) were purchased from Takara Bio (Shiga, Japan). All other reagents used in this study were of the highest grade available commercially.

2.2. Animals

Seven-week-old male Wistar rats (190-210 g) were purchased from Japan SLC, Inc. (Shizuoka, Japan). All animal experiments were evaluated and approved by the Animal and Ethics Review Committee of Tokushima University.

2.3. Preparation of psoriasis model rats

Psoriasis model rats were prepared as previously reported (Fukuta et al., 2020; Satake et al., 2018). Briefly, rats were anesthetized and maintained with 3% and 1.5% isoflurane, respectively. The dorsal skins of the rats were shaved, and 60 mg of imiquimod (IMQ) cream (Beselna cream 5%; 3 mg equivalent as IMQ) was topically applied onto a 6-cm^2 region of the dorsal skin, after which the rats were allowed to recover from anesthesia. IMQ treatment was conducted four times per 24 h to induce psoriasis, and the psoriasis model rats were used in the following experiments. To confirm induction of psoriasis, the skin of the rats was removed 24 h after the 4^{th} IMQ treatment and embedded in OCT compound, followed by freezing with dry ice/ethanol. Frozen skin sections were cut into 10-μm thick sections using a cryostat (CM3050S; Leica Biosystems, Tokyo, Japan). Thereafter, hematoxylin-eosin (HE) staining was performed to observe epidermis hyperplasia, a distinct symptom of psoriasis, as described below (2.4. HE staining of rat skin).

2.4. HE staining of rat skin

The prepared 10-μm frozen skin sections as described above (2.3. Preparation of psoriasis model rats) were fixed with 4% PFA for 10 min in humidified chamber. After washing with phosphate-buffered saline (PBS), the sections were stained with Mayer's hematoxylin solution for 10 min at room temperature, washed with distilled water, and subsequently stained with 1% eosin Y solution for 1 min at room temperature. The sections were then dehydrated with 80–100% ethanol, cleared with xylene, and mounted with hydrophobic mounting medium (Entellan New®). Thereafter, the sections were observed with a fluorescence phase contrast microscope (BZ-9000, Keyence, Osaka, Japan).

2.5. Iontophoresis (IP)

IP of NF-κB decoy-ODN and the AT1002 analog was performed in accordance with our

previous report with slight modifications (Fukuta et al., 2020; Hama et al., 2014). Briefly, Wistar rats were anesthetized by intraperitoneal injection of chloral hydrate (400 mg/kg rat) dissolved in PBS, and the dorsal skin of the rats was shaved with a hair shaver. PBS used in the present study was composed of 137 mM NaCl, 2.7 mM KCl, 10 mM $Na_2HPO_4 \cdot 12H_2O$, and 1.8 mM KH_2PO_4. For administration of FAM-ODN, nonwoven fabric (1 cm^2) containing 10 μg (in 100 μL RNase free water) of ODN solution was placed on the dorsal skin, and a nonwoven fabric (1 cm^2) moistened with 100 μL of PBS was also placed 1 cm away. Each nonwoven fabric containing ODN or PBS was attached to a Ag-AgCl electrode (3M Health Care, Minneapolis, MN, USA) with a surface area of 1 cm^2. The Ag-AgCl electrodes with nonwoven fabric containing ODN or PBS were connected to the cathode and anode of a power supply (TTI ellebeau Inc., model TCCR-3005, Tokyo, Japan), respectively. The connections were covered with tape, and IP was then performed with a constant current of 0.34 mA/cm^2 (0.34 mA) for 1 h.

For pretreatment of the skin with the AT1002 analog, nonwoven fabric (1 cm^2) containing 1058 μg of the AT1002 analog (in 100 μL deionized distilled water; 400 μg equivalent as AT1002) was attached to the Ag-AgCl electrode, and the electrode was connected to the anode of the power supply (Cathode: PBS), followed by 1 h of IP (0.34 mA). Pretreatment by IP administration of the AT1002 analog was performed 2 h prior to the start of IP administration of ODN, and the electrode with nonwoven fabric containing ODN was attached to the same position as that containing the AT1002 analog. Thereafter, IP was performed (0.34 mA for 1 h). To evaluate the effect of the IP-administered control 10-mer peptide, nonwoven fabric containing 400 μg of the peptide (in 100 μL deionized distilled water) was attached to the Ag-AgCl electrode, and anodal IP (0.34 mA for 1 h) was performed.

2.6. Intradermal distribution of fluorescence-labeled oligodeoxynucleotide

IP of FAM-ODN was performed in accordance with above-mentioned procedures (2.5. Iontophoresis (IP)). Immediately after 1-h IP of FAM-ODN, 10-μm frozen skin sections were

prepared as described above (2.3. Preparation of psoriasis model rats). The 10-μm thick frozen skin sections were attached to MAS-coated slide glasses and mounted with Perma Fluor Aqueous Mounting Medium. FAM fluorescence in the skin sections was observed using a confocal laser scanning microscope (LSM700, Carl Zeiss, Jena, Germany). Average delivery depth of FAM-ODN from the skin surface was determined using image analysis software (NIH ImageJ), and was calculated from over 5 images per rat in each group in accordance with our previous report with slight modifications (Kajimoto et al., 2011).

2.7. Intradermal distribution of IP-administered FAM-labeled ODN in psoriatic skin

At 24 h after the 4th IMQ treatment on the dorsal skin of rats, pretreatment with IP-administered AT1002 analog (400 μg AT1002 dose in 100 μL) or with control 10-mer peptide (400 μg peptide dose in 100 μL), and IP administration of FAM-ODN (50 μg in 100 μL) was performed as described above (2.5. Iontophoresis (IP)). At 0 h after 1-h IP for FAM-ODN, the psoriatic skin was collected and frozen with dry ice/ethanol, and 10-μm frozen skin sections were prepared with a cryostat. After mounting the sections with Perma Fluor Aqueous Mounting Medium, FAM fluorescence in the skin was observed by confocal laser scanning microscopy. Average delivery depth of FAM-ODN from the psoriatic skin surface was calculated using the ImageJ software, and was calculated from over 5 images per rat in each group.

2.8. Intradermal distribution of fluorescence-labeled AT1002 analog in heathy and psoriatic skin

To evaluate intradermal distribution of FITC-labeled AT1002 analog, nonwoven fabric (1 cm^2) containing 16 (for healthy rats) or 80 μg (for psoriasis model rats) of the peptide (dissolved in 100 μL deionized distilled water) was attached to the Ag-AgCl electrode, followed by connecting to the anode of the power supply. After 0 or 2 h after 1-h IP, frozen skin sections of healthy and IMQ-treated psoriatic model rats were prepared as described above (2.6. Intradermal distribution of

fluorescence-labeled oligodeoxynucleotide), and FITC fluorescence in the skin sections was observed with a confocal laser scanning microscope.

2.9. IP of NF-κB decoy ODN in the psoriasis model

At 24 h after the 4th IMQ treatment, IMQ-induced psoriasis model rats were anesthetized with chloral hydrate (400 mg/kg rat). Nonwoven fabric (1 cm^2) containing 50 μg NF-κB decoy ODN solution (in 100 μL of RNase free water) was attached to a Ag-AgCl electrode with a surface area of 1 cm^2, and applied onto the psoriatic skin. Electrodes with nonwoven fabric containing NF-κB decoy ODN or PBS were connected to the cathode and anode of the power supply, respectively. IP was performed with a constant current of 0.34 mA/cm^2 (0.34 mA) for 1 h. For pretreatment of the psoriatic skin with the AT1002 analog, IP administration of the AT1002 analog (1058 μg in 100 μL deionized distilled water; 400 μg equivalent as AT1002) was performed as described above (2.5. Iontophoresis (IP)). At 24 h after IP treatment, the rats were euthanized, and the skin tissue of the rats under the cathode was removed and used in the following experiments.

2.10. RNA extraction

After removal of the skin tissue of the rats, RNA extraction was performed as described previously with slight modifications (Howe et al., 2018; Robbe-Saule et al., 2017). Briefly, 0.5 cm^2 of cut skin was homogenized in 4 mL of QIAzol Lysis reagent using a TissueRuptor II (QIAGEN). After 5 min incubation at room temperature, total RNA was purified and extracted with an RNeasy Plus Universal Midi Kit according to the manufacturer's instructions. The total RNA concentration was quantified using a Nanodrop 8000 (Thermo Fisher Scientific).

2.11. Quantitative analysis of mRNA expression by real-time reverse transcription polymerase chain reaction (RT-PCR)

By using extracted RNA, real-time RT-PCR was performed as described previously with

slight modifications (Shimokawa et al., 2020). Briefly, cDNA was synthesized from 200 ng of total RNA with PrimeScript RT Master Mix (Perfect Real Time) using a MJ Mini Personal Thermal Cycler (Bio-Rad, Hercules, CA, USA). The conditions for the reverse transcription reaction were 37ºC for 15 min, whereas that for inactivation of reverse transcriptase were 85ºC for 5 sec. Real-time RT-PCR analysis was performed with TB Green™ Premix Ex Taq™ II (Tli RNaseH Plus) using a Thermal Cycler Dice Real Time System III (Takara Bio). For analysis of the mRNA expression levels of TNF-α, IL-6, and GAPDH, the cDNA was denatured at 95ºC for 30 sec, followed by 40 cycles of 95ºC for 5 sec and 60ºC for 30 sec for amplification. The primers were synthesized by Eurofins Genomics, and those sequences used for the real-time RT-PCR are shown in Table 1. mRNA levels of TNF-α and IL-6 were calculated using the $2^{-\Delta\Delta Ct}$ method by normalization relative to GAPDH mRNA levels. The relative transcript levels (THN-α/GAPDH mRNA and IL-6/GAPDH mRNA) were calculated to compare the differences between each group.

2.12. Evaluation of epidermis layer thickness

Pretreatment of IP-administered AT1002 analog and IP administration of NF-κB decoy ODN were performed as mentioned above (2.9. IP of NF-κB decoy ODN in the psoriasis model) in IMQ-treated psoriasis model rats, followed by preparation of frozen skin sections 24 h IP administration of NF-κB decoy ODN. The 10-μm frozen skin tissues of each group of psoriasis model rats were stained with HE and observed using a fluorescence phase contrast microscope (BZ-9000). Average epidermis layer thickness was determined from >20 images per rat with the image analysis software of BZ-9000.

2.13. Statistical analysis

Statistical differences were evaluated by one-way analysis of variance with the Tukey post-hoc test. Data are presented as mean ± standard deviation (S.D.).

3. Results

3.1. Intradermal distribution of fluorescence-labeled oligodeoxynucleotides administered via IP in healthy and psoriatic skin

We performed transdermal delivery of FAM-ODN by IP on the dorsal skin of healthy and IMQ-treated psoriasis model rats. Images of HE staining obtained from both rats showed that epidermis hyperplasia, a symptom of psoriasis, was observed in IMQ-treated rats but not in untreated healthy rats (Figs 1A and B), indicating that psoriatic inflammation was induced by repeated topical application of IMQ cream, consistent with previous reports (Satake et al., 2018). For topical skin application of FAM-ODN, FAM fluorescence was only observed on the stratum corneum, as judged from HE staining, and hardly detected in skin tissues (Fig. 1C). No fluorescence was observed in the group receiving iontophoretic treatment alone (Fig. 1D). When FAM-ODN was administered via IP, fluorescence of FAM-ODN was clearly observed from the epidermis to the dermis layer of healthy skin at immediately after 1-h IP (Fig. 1E), consistent with our previous reports on intradermal delivery of nucleic acid therapeutics (e.g., siRNA and CpG-DNA) via IP (Kigasawa et al., 2010; Kigasawa et al., 2011). However, in IMQ-treated psoriasis model rats, IP-mediated intradermal permeation of FAM-ODN was hardly observed and fluorescence was detected only on the surface of the epidermis layer (Fig. 1F), suggesting that psoriatic skin barriers (due to epidermis hyperplasia) hampered permeation of ODN via IP. On the other hand, no obvious skin damage was observed by IP treatment both in healthy and IMQ-treated psoriasis model rats as shown in pictures of dorsal skin of the rats and the images of HE staining (Supplementary Fig. 1).

3.2. Intradermal delivery of NF-κB decoy ODN into thickened psoriatic skin via IP combined with the AT1002 analog

As transdermal permeation of FAM-ODN could not be achieved by IP alone, we sought to overcome the thickened psoriatic skin barrier by a combination of IP and the tight junction-opening

peptide AT1002 (Phe-Cys-Ile-Gly-Arg-Leu). As the electric charge of AT1002 is nearly neutral (or weakly positive), the delivery efficiency of AT1002 via IP was considered to be low. Hence, to make the physicochemical property of AT1002 more suitable for IP, we designed an AT1002 analog (Arg-Arg-Arg-Gly-Gly-Phe-Cys-Ile-Gly-Arg-Leu), in which the AT1002 peptide was ligated with two Gly spacers and three Arg residues (positively charged moieties). At first, we prepared a complex of FAM-ODN and the AT1002 analog via electrostatic interaction and subsequently performed IP of the complex. However, intradermal permeation of the complex could not be observed, even in healthy skin (data not shown). We then examined the effect of pretreatment by IP administration of the AT1002 analog on the intradermal delivery efficiency of FAM-ODN. To determine the appropriate timing of IP treatment with the AT1002 analog prior to FAM-ODN IP, we performed IP of the AT1002 analog at different time points, namely 1, 3, or 6 h prior to FAM-ODN IP, using healthy rats. For these experiments, electrodes with nonwoven fabric containing the AT1002 analog and FAM-ODN were set at the same skin positions. Results of these preliminary experiments showed that, although transdermal permeation of FAM-ODN tended to increase by the pretreatment with AT1002 analog IP performed 1 or 6 h before the start of FAM-ODN IP, significant increase in permeation of FAM-ODN was observed following pretreatment with the AT1002 analog at 3 h prior to the start of FAM-ODN IP (Supplementary Fig. 2). Thus, we decided to carry out pretreatment with the AT1002 analog IP at 3 h prior to the start of IP of FAM-ODN, as shown in Fig. 2A. Confocal microscopic images of healthy skin treated with a combination of IP with the AT1002 analog and FAM-ODN showed that FAM fluorescence was more broadly and brightly observed compared with IP alone (Figs. 2B and D). Moreover, the depth of FAM-ODN delivery was significantly increased (2.9-fold) by a combination of IP with the AT1002 analog (Fig. 2E). On the other hand, in the group of pretreatment with the control 10-mer peptide (Arg-Arg-Arg-Gly-Gly-Leu-Gly-Cys-Arg-Phe-Ile), FAM fluorescence in the skin of healthy rats was almost similar to the group of FAM ODN IP alone (Fig. 2C). The quantitative analysis of penetration depth also showed that the pretreatment with IP of the control 10-mer peptide hardly affected the permeation of FAM-ODN (Fig. 2E), indicating that

enhancement of intradermal delivery of FAM-ODN was derived from the pretreatment with IP of the tight junction opening peptide AT1002.

Based on the results using healthy rats, we next investigated the combination IP system in IMQ-treated psoriasis model rats according to the experimental schedule shown in Fig. 2F. Similar to the results shown in Fig. 1F, efficient transdermal permeation of FAM-ODN was not observed in the group treated with IP alone (Fig. 2G). Also, the combination of FAM-ODN IP and pretreatment with the control peptide IP could not achieve efficient delivery of FAM-ODN into the psoriatic thickened skin (Fig. 2H). However, in the case of the combination of FAM-ODN IP and pretreatment with AT1002 analog IP, FAM fluorescence was broadly observed in the psoriatic skin, and also reached the dermis layer (Fig. 2I). Quantitative data on the depth of delivery of the ODN also indicated significant (7.8-fold) enhancement of intradermal permeation of FAM-ODN by a combination of IP and AT1002 analog pretreatment (Fig. 2J).

3.3. Intradermal distribution of IP-administered fluorescence-labeled AT1002 analog in heathy and psoriasis model rats

By using FITC-labeled AT1002 analog, intradermal distribution of IP-administered AT1002 analog in healthy and psoriasis model rats was investigated. In healthy rats, the FITC fluorescence was observed from the epidermis to the dermis layer of healthy skin at immediately after 1-h IP (Fig. 3A). The fluorescence of the peptide remained in the epidermis and dermis layers 2 h after 1-h IP, namely at the timing of FAM-ODN IP (Fig. 3B). On the other hand, the FITC fluorescence was mainly observed in the thickened epidermis layer of the IMQ-treated psoriasis model rats at 0 h after 1-h IP (Fig. 3C). Importantly, the FITC-labeled AT1002 analog reached the dermis layer of the psoriatic skin 2 h after IP administration of the peptide (Fig. 3D).

3.4. Suppression of upregulation of inflammatory cytokine mRNA by combined IP treatment with NF-κB decoy ODN and the AT1002 analog

We investigated the biological function of NF-κB decoy ODN delivered into psoriatic skin via a combination of IP and AT1002 analog pretreatment. As NF-κB decoy ODN can inhibit transcriptional induction of various inflammatory cytokines (e.g., TNF-α, IL-6) via the transcriptional factor NF-κB, we evaluated the effect of IP-administered NF-κB decoy ODN on mRNA levels of TNF-α and IL-6. IP administration of NF-κB decoy ODN was performed on the psoriatic skin at 24 h after the 4th IMQ treatment, and mRNA levels of TNF-α and IL-6 were assessed at 24 h after IP, as shown in Fig. 4A. Results showed that IMQ treatment significantly increased mRNA levels of TNF-α and IL-6 in the skin of the psoriasis model rats (Figs. 4B and C). IP of NF-κB decoy ODN had almost no effect on TNF-α mRNA levels compared with IMQ-treated rats (Fig. 4B), while IL-6 mRNA levels tended to decrease (Fig. 4C). On the other hand, in the group receiving a combination of NF-κB decoy IP and pretreatment with AT1002 analog IP, TNF-α mRNA levels were significantly decreased (Fig. 4B). Moreover, the combination exhibited superior suppressive effects on IL-6 mRNA levels compared with the group receiving NF-κB decoy ODN IP alone (Fig. 4C).

3.5. Therapeutic effect of combined IP delivery of NF-κB decoy ODN and the AT1002 analog on psoriasis

Finally, we investigated the therapeutic effect of combined IP delivery of NF-κB decoy ODN and the AT1002 analog in IMQ-induced psoriasis model rats by evaluating epidermis thickness as an indicator of epidermis hyperplasia after psoriatic inflammation. Images of HE staining showed that four IMQ treatments significantly increased epidermis thickness compared to untreated normal rats (Figs. 5A, B, and E). IP administration of NF-κB decoy ODN had almost no effect on epidermis hyperplasia compared with IMQ-treated rats (Figs. 5C and E). On the other hand, IP of NF-κB decoy ODN combined with pretreatment with IP-administered AT1002 analog significantly ameliorated epidermis hyperplasia compared with IMQ-treated rats and rats receiving NF-κB decoy ODN IP alone (Figs. 5D and E).

4. Discussion

Our previous studies demonstrated the utility of IP using weak electric current (0.3–0.5 mA/cm^2) to enable intradermal delivery of hydrophilic macromolecules, such as nucleic acid therapeutics, antibodies, and nanoparticles (Fukuta et al., 2020; Kajimoto et al., 2011; Kigasawa et al., 2010). Based on the results of mechanistic studies, we found that IP-induced Ca^{2+} influx and protein kinase C-α activation is related to the cleavage of intercellular junctions via gap junction dissociation by connexin 43 reduction and depolymerization of filamentous actin (Hama et al., 2014). However, under psoriasis conditions, the thickened pathological skin barrier exhibiting broad localization of tight junction proteins hampered intradermal permeation of IP-administered macromolecule drugs in our previous study (Fukuta et al., 2020). Moreover, in the present study, IP-administered FAM-ODN was unable to penetrate the thickened psoriatic skin, but was found to efficiently permeate the skin of healthy rats (Fig. 1). Hence, to achieve efficient delivery of macromolecules (including nucleic acid therapeutics), combination of IP with treatments capable of regulating intercellular junctions is required to overcome the psoriatic skin barrier.

To this end, we focused on the functional peptide AT1002 (Phe-Cys-Ile-Gly-Arg-Leu) to regulate tight junction in the skin. AT1002 was reported to exhibit tight junction-opening abilities (Goldblum et al., 2011; Uchida et al., 2011b). Combination of AT1002 with IP was expected to allow for synergistic effects of tight junction-opening activity associated with AT1002 and the intercellular cleavable effect of IP. Also, as weak electric current employed for IP can evoke endocytosis with unique properties that allow for easy leakage of substances with molecular weights <70,000 (Hasan et al., 2016b; Torao et al., 2020), intradermally delivered nucleic acid therapeutics may be efficiently taken up by the inflamed skin cells, and subsequently reach the cytoplasm to exert the functions.

We evaluated the combination effect of IP and pretreatment with IP of the AT1002 analog (Arg-Arg-Arg-Gly-Gly-Phe-Cys-Ile-Gly-Arg-Leu) on the intradermal delivery efficiency of FAM-ODN. The AT1002 analog containing positively charged moieties was designed to facilitate IP application of the peptide to deeply penetrate the skin. As shown in Figure 1, IP alone could deliver

FAM-ODN into the skin of healthy rats, whereas the combination of pretreatment with the AT1002 analog IP was found to significantly enhance (2.9-fold) intradermal permeation of FAM-ODN (Figs. 2A-E). In IMQ-treated psoriasis model rats, transdermal permeation of FAM-ODN was not observed upon treatment with IP alone (Fig. 2G). Surprisingly, the fluorescence of FAM extended from the thickened epidermis layer to the dermis layer by a combination of FAM-ODN IP and AT1002 analog pretreatment IP (Figs. 2I and J), indicating that the combination system could overcome the thickened psoriatic skin barrier and allow for intradermal permeation of nucleic acid therapeutics. On the other hand, the combination of FAM-ODN IP and pretreatment with IP of the control 10-mer peptide (Arg-Arg-Arg-Gly-Gly-Leu-Gly-Cys-Arg-Phe-Ile), which peptide was designed with three Arg and two Gly spacers without the sequences of the tight junction opening peptide AT1002, could not enhance transdermal permeation of FAM-ODN into both healthy and psoriatic thickened skins (Figs. 2C, E, H, J). These results indicate that enhancement of intradermal delivery of FAM-ODN was derived from the pretreatment with IP of AT1002 analog. It was previously reported that abnormal tight junctions associated with epidermal cell proliferation are formed in the psoriatic skin, and that expression of tight junction-related proteins, including occludin and ZO-1, extends to the stratum spinosum, which proteins are normally localized in the stratum granulosum (Kirschner et al., 2009). Also, keratinocytes in the epidermis of psoriatic skin were reported to be highly proliferative due to certain inflammatory cytokines, which leads to immune cell migration and epidermis hyperplasia (Lowes et al., 2007). Considering these findings and the results of the present study, it was suggested that a combination of weak electricity and the AT1002 analog could synergistically affect the state of the skin barrier composed of both abnormal tight junctions and proliferated cells via intercellular junction cleaving and tight junction-opening effects, respectively.

In the present study, we newly designed the AT1002 analog (Arg-Arg-Arg-Gly-Gly-Phe-Cys-Ile-Gly-Arg-Leu) to make the physicochemical property of AT1002 more applicable for IP. Since application of IP for the original AT1002 (Phe-Cys-Ile-Gly-Arg-Leu) with insufficient charged residues is difficult and the effect of the original AT1002 cannot be

compared with the AT1002 analog, it is thought to be impossible to directly evaluate whether the activity of the AT1002 analog is the same as the original AT1002. However, in the present study, IP administration of the AT1002 analog promoted intradermal permeation of IP-administered FAM-ODN not only in healthy skin but also in psoriatic skin (Fig. 2). Therefore, it is considered that the designed AT1002 analog could have a similar tight junction-opening effect to the original AT1002.

From the experiments to decide the time schedule of pretreatment with AT1002 analog IP, although the pretreatment with the AT1002 analog IP at 1 or 6 h prior to the start of FAM-ODN IP tended to enhance FAM-ODN permeation into the skin, the pretreatment done 3 h prior to FAM-ODN IP significantly increased intradermal permeation of FAM-ODN (Supplementary Figure 2). Based on these results, it was considered that certain time was needed for intradermally delivered AT1002 analog to exert its tight junction-opening activity to cause skin barrier function change, which change is enough to enable efficient intradermal permeation of the subsequently administered ODN. On the other hand, based on our previous reports regarding IP-mediated successful delivery of nucleic acid therapeutics (Kigasawa et al., 2010; Kigasawa et al., 2011) and considering the risk of skin burn and other adverse effects, we performed IP of the AT1002 analog and ODN for 1 h in this study.

Intradermal distribution of IP-administered AT1002 analog was also evaluated by using FITC-labeled AT1002 analog. The FITC fluorescence was extended from the epidermis to the dermis layer of healthy skin before the timing of IP administration of FAM-ODN (Figs. 3A and B). Although the FITC-labeled AT1002 analog was mainly distributed in the thickened epidermis layer immediately after 1- h IP, its fluorescence reached the dermis layer of the psoriatic skin at 2 h after 1-h IP (Figs. 3C and D). These results suggest that the AT1002 analog administered via IP could exert its tight-junction opening activity and affect the state of the skin barrier of both healthy and psoriasis model rats. Consequently, it is suggested that the AT1002 analog pretreatment could

promote transdermal permeation of subsequently administered FAM-ODN, resulting in overcoming aberrant psoriatic thickened skin barrier.

Under psoriatic conditions, upregulation of several inflammatory cytokines, including TNF-α and IL-6, is induced by NF-κB activation. Indeed, mRNA levels of both TNF-α and IL-6 were significantly increased in the dorsal skin of IMQ-treated psoriasis model rats (Fig. 4). IP administration of a single dose of NF-κB decoy ODN hardly affected mRNA levels of both cytokines. On the other hand, intradermal delivery of NF-κB decoy ODN by a combination of IP and AT1002 analog pretreatment significantly reduced the levels of TNF-α mRNA and tended to decrease levels of IL-6 mRNA (Fig. 4B and C), suggesting that pretreatment with the AT1002 analog enabled efficient delivery of IP-delivered NF-κB decoy ODN and subsequent exertion of its function. For proper functioning of NF-κB decoy ODN, ODN needs to be taken up into the target cells and subsequently reach the cytoplasm. We previously reported that the weak electric current treatment used for IP can induce a unique endocytosis process to result in subsequent cytoplasmic delivery of nucleic acid therapeutics via activation of specific cellular signaling (Hasan et al., 2019). Therefore, it is suggested that IP may allow for not only intradermal delivery of NF-κB decoy ODN by combination with AT1002, but also for cytoplasmic delivery via weak electric current-induced unique endocytosis, resulting in suppression of upregulation of mRNA levels of inflammatory cytokines in psoriatic skin.

Finally, we evaluated therapeutic outcomes of IMQ-induced psoriasis model rats by treatment with NF-κB decoy ODN IP combined with pretreatment by AT1002 analog IP. IMQ treatment significantly induced epidermal hyperplasia, which was correlated with upregulation of levels of TNF-α and IL-6 mRNA (Figs. 5A, B, E). Although intradermal delivery of the ODN via IP alone hardly decreased the thickness of the epidermis, the ODN delivered by a combination of IP and AT1002 analog pretreatment significantly suppressed epidermal hyperplasia compared with the untreated group (Figs. 5C-E). It was previously reported that NF-κB signaling plays a crucial role in the progression of psoriasis pathology (Goldminz et al., 2013; Stratis et al., 2006; Xiao et al., 2017).

Under psoriasis conditions, activation of NF-κB signaling is induced in intradermal macrophages and keratinocytes, and leads to release of TNF-α and IL-6 from those cells, resulting in subsequent activation of Langerhans cells (a subset of dendritic cell) and T cells. Then, several inflammatory cytokines secreted from the activated cells further activate keratinocytes, and the pathology of psoriasis is exacerbated. In the present study, intradermal delivery of NF-κB decoy ODN via combination IP could suppress upregulation of mRNA levels of TNF-α and IL-6 in IMQ-treated psoriasis model rats. These results, combined with the findings from previous reports, suggest that inhibition of NF-κB signaling by the decoy ODN could suppress a series of immune reactions, resulting in amelioration of epidermal hyperplasia. Based on these results, it is suggested that intradermal delivery of NF-κB decoy ODN via IP combined with AT1002 analog pretreatment could be useful for the treatment of psoriasis.

To exert the functionality of the NF-κB decoy ODN, its stability in the skin and influence of the IP treatment on the stability are needed to be considered. In the present study, NF-κB decoy ODN intradermally delivered by combination with AT1002 analog IP pretreatment showed significant therapeutic effect in IMQ-treated psoriasis model rats. Also, in our previous studies, we succeeded in intradermal delivery of other nucleic acid therapeutics siRNA and CpG-ODN into the skin and exertion of their respective effects, namely target mRNA knockdown effect and induction of immune responses against cancer (Kigasawa et al., 2010; Kigasawa et al., 2011). These results suggest that the intradermally delivered ODN could be stable in the psoriatic skin and exert its function. Although the period of the ODN been stable in the skin is unclear, weak electric current was previously found to rapidly induce a unique endocytosis which can leak substances with molecular weights <70,000 (Hasan et al., 2016; Torao et al., 2020). It is considered that the IP-delivered ODN could be taken up via the unique endocytosis and delivered in the cytoplasm of skin cells before degradation in the skin tissue. In addition, our previous reports demonstrated cytoplasmic delivery of siRNA via weak electric current treatment without loss of the activity of siRNA in *in vitro* (Hasan et al., 2016; Hasan

et al., 2019). Based on these findings, it is suggested that the IP treatment should not affect the ODN stability.

In the present study, we demonstrated efficient intradermal delivery of NF-κB decoy ODN by overcoming the thickened pathological skin barrier via synergistic effects of IP and AT1002 analog pretreatment, and successfully achieved treatment of psoriasis. The high costs and undesirable adverse side effects (resulting from frequent administrations) associated with nucleic acid therapeutics are major challenges for their use in the treatment of diseases (Brezinski et al., 2015; Miller and Pisani, 1999). In this study, single administration of NF-κB decoy ODN by the combination IP system was shown to effectively decrease mRNA levels of inflammatory cytokines and ameliorate psoriasis symptoms in IMQ-treated model rats. Hence, IP combined with the AT1002 analog is expected to realize non-invasive and efficient intradermal delivery of nucleic acid therapeutics and reduce dosage and frequency of administration, which may lead to improvement of quality of life in patients suffering from psoriasis. For transdermal delivery of hydrophilic macromolecules including nucleic acid therapeutics, low bioavailability is known as one of the serious problems (Levin et al., 2005; Seong et al., 2017). Since combination of pretreatment with AT1002 analog and NF-κB decoy ODN could enhance transdermal permeation of IP-administered ODN and its therapeutic efficacy in psoriasis model rats, the combination IP system employed in the present study is considered to increase the bioavailability of ODN after IP treatment compared with IP alone. Although we used NF-κB decoy ODN as a representative nucleic acid therapeutic in the present study, we previously demonstrated successful delivery of other macromolecular drugs, such as antibodies, siRNA, etc. Results of the present study suggest that application of a combination IP system with the AT1002 analog can increase the therapeutic efficacy of such macromolecular drugs.

5. Conclusions

In summary, results of the present study demonstrate the utility of a combination of IP and the tight junction-opening peptide AT1002 to overcome the thickened psoriatic skin barrier to enable efficient intradermal delivery of nucleic acid therapeutics for the treatment of psoriasis. Pretreatment of skin with IP-administered AT1002 analog could enhance transdermal delivery of FAM-ODN via IP. Moreover, the delivered ODN broadly extended from the epidermis to the dermis layers of psoriatic skin; although FAM-ODN was found to distribute on the surface of the epidermis in the group receiving IP alone. Intradermal administration of NF-κB decoy ODN via IP combined with AT1002 analog pretreatment significantly suppressed IMQ-induced upregulation of mRNA levels of TNF-α and IL-6, which cytokines are related to pathological progression of psoriasis. Moreover, NF-κB decoy ODN delivered via IP combined with the AT1002 analog significantly ameliorated epidermis hyperplasia in psoriasis model rats. Taken together, these results suggest that combination of IP with the AT1002 analog could synergistically affect the state of the thickened psoriatic skin barrier to achieve transdermal delivery of NF-κB ODN into the inflamed skin, and that intradermal delivery of NF-κB decoy ODN by the combination IP system could be useful for the treatment of psoriasis.

Acknowledgements

This research was supported by the Research Program for the Development of Intelligent Tokushima Artificial Exosome (iTEX) from Tokushima University.

Declaration of interest statement

The authors declare no competing financial interests.

References

Anselmo, A.C., Gokarn, Y., Mitragotri, S., 2019. Non-invasive delivery strategies for biologics. Nat Rev Drug Discov 18, 19-40.

Banga, A.K., Prausnitz, M.R., 1998. Assessing the potential of skin electroporation for the delivery of protein-and gene-based drugs. Trends Biotechnol 16, 408-412.

Brezinski, E.A., Dhillon, J.S., Armstrong, A.W., 2015. Economic burden of psoriasis in the United States: a systematic review. JAMA Dermatol 151, 651-658.

Dharamdasani, V., Mandal, A., Qi, Q.M., Suzuki, I., Bentley, M., Mitragotri, S., 2020. Topical delivery of siRNA into skin using ionic liquids. J Control Release 323, 475-482.

Fukuta, T., Oshima, Y., Michiue, K., Tanaka, D., Kogure, K., 2020. Non-invasive delivery of biological macromolecular drugs into the skin by iontophoresis and its application to psoriasis treatment. J Control Release 323, 323-332.

Gilmore, T.D., Garbati, M.R., 2010. Inhibition of NF-κB signaling as a strategy in disease therapy. NF-kB in Health and Disease, 245-263.

Goldblum, S.E., Rai, U., Tripathi, A., Thakar, M., De Leo, L., Di Toro, N., Not, T., Ramachandran, R., Puche, A.C., Hollenberg, M.D., Fasano, A., 2011. The active Zot domain (aa 288-293) increases ZO-1 and myosin 1C serine/threonine phosphorylation, alters interaction between ZO-1 and its binding partners, and induces tight junction disassembly through proteinase activated receptor 2 activation. FASEB J 25, 144-158.

Goldminz, A.M., Au, S.C., Kim, N., Gottlieb, A.B., Lizzul, P.F., 2013. NF-kappaB: an essential transcription factor in psoriasis. J Dermatol Sci 69, 89-94.

Guy, R.H., Kalia, Y.N., Delgado-Charro, M.B., Merino, V., López, A., Marro, D., 2000. Iontophoresis: electrorepulsion and electroosmosis. J Control Release 64, 129-132.

Hama, S., Kimura, Y., Mikami, A., Shiota, K., Toyoda, M., Tamura, A., Nagasaki, Y., Kanamura, K., Kajimoto, K., Kogure, K., 2014. Electric stimulus opens intercellular spaces in skin. J Biol Chem 289, 2450-2456.

Hasan, M., Hama, S., Kogure, K., 2019. Low Electric Treatment activates Rho GTPase via Heat Shock Protein 90 and Protein Kinase C for Intracellular Delivery of siRNA. Sci Rep 9, 4114.

Hasan, M., Khatun, A., Fukuta, T., Kogure, K., 2020. Noninvasive transdermal delivery of liposomes by weak electric current. Adv Drug Deliv Rev 154-155, 227-235.

Hasan, M., Nishimoto, A., Ohgita, T., Hama, S., Kashida, H., Asanuma, H., Kogure, K., 2016a. Faint electric treatment-induced rapid and efficient delivery of extraneous hydrophilic molecules into the cytoplasm. J Control Release 228, 20-25.

Hasan, M., Tarashima, N., Fujikawa, K., Ohgita, T., Hama, S., Tanaka, T., Saito, H., Minakawa, N., Kogure, K., 2016b. The novel functional nucleic acid iRed effectively regulates target genes following cytoplasmic delivery by faint electric treatment. Sci Technol Adv Mater 17, 554-562.

Hashim, II, Motoyama, K., Abd-Elgawad, A.E., El-Shabouri, M.H., Borg, T.M., Arima, H., 2010. Potential use of iontophoresis for transdermal delivery of NF-kappaB decoy oligonucleotides. Int J Pharm 393, 127-134.

Hawkes, J.E., Chan, T.C., Krueger, J.G., 2017. Psoriasis pathogenesis and the development of novel targeted immune therapies. J Allergy Clin Immunol 140, 645-653.

Howe, C., Kim, S.J., Mitchell, J., Im, E., Kim, Y.S., Kim, Y.S., Rhee, S.H., 2018. Differential expression of tumor-associated genes and altered gut microbiome with decreased Akkermansia muciniphila confer a tumor-preventive microenvironment in intestinal epithelial Pten-deficient mice. Biochim Biophys Acta Mol Basis Dis 1864, 3746-3758.

Isomura, I., Morita, A., 2006. Regulation of NF‐κB Signaling by Decoy Oligodeoxynucleotides. Microbiol Immunol 50, 559-563.

Kajimoto, K., Yamamoto, M., Watanabe, M., Kigasawa, K., Kanamura, K., Harashima, H., Kogure, K., 2011. Noninvasive and persistent transfollicular drug delivery system using a combination of liposomes and iontophoresis. Int J Pharm 403, 57-65.

Kigasawa, K., Kajimoto, K., Hama, S., Saito, A., Kanamura, K., Kogure, K., 2010. Noninvasive delivery of siRNA into the epidermis by iontophoresis using an atopic dermatitis-like model rat. Int J

Pharm 383, 157-160.

Kigasawa, K., Kajimoto, K., Nakamura, T., Hama, S., Kanamura, K., Harashima, H., Kogure, K., 2011. Noninvasive and efficient transdermal delivery of CpG-oligodeoxynucleotide for cancer immunotherapy. J Control Release 150, 256-265.

Kirschner, N., Poetzl, C., von den Driesch, P., Wladykowski, E., Moll, I., Behne, M.J., Brandner, J.M., 2009. Alteration of tight junction proteins is an early event in psoriasis: putative involvement of proinflammatory cytokines. Am J Pathol 175, 1095-1106.

Lark, M.R., Gangarosa Sr, L.P., 1990. Iontophoresis: an effective modality for the treatment of inflammatory disorders of the temporomandibular joint and myofascial pain. CRANIO® 8, 108-119.

Levin, G., Gershonowitz, A., Sacks, H., Stern, M., Sherman, A., Rudaev, S., Zivin, I., Phillip, M., 2005. Transdermal delivery of human growth hormone through RF-microchannels. Pharm Res 22, 550-555.

Lowes, M.A., Bowcock, A.M., Krueger, J.G., 2007. Pathogenesis and therapy of psoriasis. Nature 445, 866-873.

Mandal, A., Kumbhojkar, N., Reilly, C., Dharamdasani, V., Ukidve, A., Ingber, D.E., Mitragotri, S., 2020. Treatment of psoriasis with NFKBIZ siRNA using topical ionic liquid formulations. Sci Adv 6, eabb6049.

Mikszta, J.A., Alarcon, J.B., Brittingham, J.M., Sutter, D.E., Pettis, R.J., Harvey, N.G., 2002. Improved genetic immunization via micromechanical disruption of skin-barrier function and targeted epidermal delivery. Nat Med 8, 415-419.

Miller, M., Pisani, E., 1999. The cost of unsafe injections. Bull World Health Organ 77, 808.

Prausnitz, M.R., Langer, R., 2008. Transdermal drug delivery. Nat Biotechnol 26, 1261-1268.

Robbe-Saule, M., Babonneau, J., Sismeiro, O., Marsollier, L., Marion, E., 2017. An optimized method for extracting bacterial RNA from mouse skin tissue colonized by Mycobacterium ulcerans. Front Microbiol 8, 512.

Satake, K., Amano, T., Okamoto, T., 2018. Low systemic exposure and calcemic effect of

calcipotriol/betamethasone ointment in rats with imiquimod-induced psoriasis-like dermatitis. Eur J Pharmacol 826, 31-38.

Seong, K.-Y., Seo, M.-S., Hwang, D.Y., O'Cearbhaill, E.D., Sreenan, S., Karp, J.M., Yang, S.Y., 2017. A self-adherent, bullet-shaped microneedle patch for controlled transdermal delivery of insulin. J Control Release 265, 48-56.

Shimokawa, T., Fukuta, T., Inagi, T., Kogure, K., 2020. Protective effect of high-affinity liposomes encapsulating astaxanthin against corneal disorder in the in vivo rat dry eye disease model. J Clin Biochem Nutr 66, 224-232.

Song, K.H., Fasano, A., Eddington, N.D., 2008a. Effect of the six-mer synthetic peptide (AT1002) fragment of zonula occludens toxin on the intestinal absorption of cyclosporin A. Int J Pharm 351, 8-14.

Song, K.H., Fasano, A., Eddington, N.D., 2008b. Enhanced nasal absorption of hydrophilic markers after dosing with AT1002, a tight junction modulator. Eur J Pharm Biopharm 69, 231-237.

Spierings, E.L., Brevard, J.A., Katz, N.P., 2008. Two-minute skin anesthesia through ultrasound pretreatment and iontophoretic delivery of a topical anesthetic: a feasibility study. Pain Med 9, 55-59.

Stratis, A., Pasparakis, M., Rupec, R.A., Markur, D., Hartmann, K., Scharffetter-Kochanek, K., Peters, T., van Rooijen, N., Krieg, T., Haase, I., 2006. Pathogenic role for skin macrophages in a mouse model of keratinocyte-induced psoriasis-like skin inflammation. J Clin Invest 116, 2094-2104.

Tonel, G., Conrad, C., 2009. Interplay between keratinocytes and immune cells—recent insights into psoriasis pathogenesis. Int J Biochem Cell Biol 41, 963-968.

Torao, T., Mimura, M., Oshima, Y., Fujikawa, K., Hasan, M., Shimokawa, T., Yamazaki, N., Ando, H., Ishida, T., Fukuta, T., Tanaka, T., Kogure, K., 2020. Characteristics of unique endocytosis induced by weak current for cytoplasmic drug delivery. Int J Pharm 576, 119010.

Toyoda, M., Hama, S., Ikeda, Y., Nagasaki, Y., Kogure, K., 2015. Anti-cancer vaccination by transdermal delivery of antigen peptide-loaded nanogels via iontophoresis. Int J Pharm 483, 110-114.

Uchida, T., Kanazawa, T., Kawai, M., Takashima, Y., Okada, H., 2011a. Therapeutic effects on atopic

dermatitis by anti-RelA short interfering RNA combined with functional peptides Tat and AT1002. J Pharmacol Exp Ther 338, 443-450.

Uchida, T., Kanazawa, T., Takashima, Y., Okada, H., 2011b. Development of an efficient transdermal delivery system of small interfering RNA using functional peptides, Tat and AT-1002. Chem Pharm Bull 59, 196-201.

Veilleux, M.S., Shear, N.H., 2017. Biologics in patients with skin diseases. J Allergy Clin Immunol 139, 1423-1430.

Watts, T., Berti, I., Sapone, A., Gerarduzzi, T., Not, T., Zielke, R., Fasano, A., 2005. Role of the intestinal tight junction modulator zonulin in the pathogenesis of type I diabetes in BB diabetic-prone rats. Proc Natl Acad Sci U S A 102, 2916-2921.

Xiao, C., Zhu, Z., Sun, S., Gao, J., Fu, M., Liu, Y., Wang, G., Yao, X., Li, W., 2017. Activation of Langerhans cells promotes the inflammation in imiquimod-induced psoriasis-like dermatitis. J Dermatol Sci 85, 170-177.

Figure legends

Fig. 1. Intradermal distribution of IP-administered fluorescence-labeled oligodeoxynucleotides in healthy and psoriatic skin

Images of dorsal skin of healthy (A) and IMQ-treated psoriasis model rats (B) stained with HE. Stratum corneum, epidermis, and dermis layers are indicated. Confocal images of frozen skin sections (10 μm) of rats topically applied with FAM-ODN (IP (-)) for 1 h (C) and immediately after treatment by IP (0.34 mA for 1 h) with PBS (D). FAM-ODN was transdermally administered into healthy (E) or IMQ-treated psoriasis model rats (F) via IP. Immediately after IP, FAM fluorescence was observed with a confocal microscope (C; FAM-ODN (IP (-)), D; PBS IP (+), E; FAM-ODN IP (+) in healthy rats, F; FAM-ODN IP (+) in psoriasis model rats). Scale bars = 100 μm. Experiments were independently performed three times, and each experiment showed similar profiles.

Fig. 2. Intradermal distribution of NF-κB decoy ODN in thickened psoriatic skin delivered via IP combined with the AT1002 analog

FAM-ODN IP and pretreatment with AT1002 analog IP were performed for healthy rats as shown in the experimental schedule (A). Immediately after IP, FAM fluorescence was observed in the skin of the group receiving IP alone (B), IP combined with the control 10-mer peptide (C), and IP combined with the AT1002 analog pretreatment group (D). Average delivery depths of FAM-ODN from the skin surface of healthy rats (E). The psoriasis model rats were prepared by topical application of IMQ cream (60 mg/rat/treatment) for a total of four times. At 24 h after the 4^{th} IMQ treatment, each IP was performed, followed by preparation of frozen skin sections (10 μm) immediately after 1-h IP (F). Confocal images of FAM-ODN IP alone (G), IP combined with the control 10-mer peptide (H), and FAM-ODN IP combined with AT1002 analog pretreatment (I). Average delivery depths of FAM-ODN from the psoriatic skin surface (J). Scale bars = 100 μm. Data are mean ± S.D. (n=3). ** P<0.01, *** P<0.001.

Fig. 3. Intradermal distribution of fluorescence-labeled AT1002 analog administered via IP in healthy and psoriasis model rats.

Healthy (A: 0 h after 1-h IP, B: 2 h after 1-h IP) and IMQ-treated psoriasis model (24 h after 4th IMQ treatment; C: 0 h after 1-h IP, D: 2 h after 1-h IP) rats were transdermally FITC-labeled AT1002 analog by IP (0.34 mA for 1 h). At 0 or 2 h after 1-h IP, frozen skin sections (10 μm) were prepared, and the FITC fluorescence in skins were observed by confocal laser scanning microscopy. Scale bars = 100 μm.

Fig. 4. Effects of NF-κB decoy ODN delivered by a combination of IP and AT1002 analog pretreatment on inflammatory cytokine mRNA levels.

IMQ-treated psoriasis model rats were transdermally administered NF-κB decoy ODN (50 μg dose/rat) or PBS by IP (0.34 mA for 1 h) at 24 h after the 4th IMQ treatment (A). For the group receiving IP combined with the AT1002 analog, pretreatment with IP of the AT1002 analog (400 μg AT1002 dose; 0.34 mA for 1 h) was performed 3 h prior to the start of ODN administration. Twenty-four hours after IP of NF-κB decoy ODN, mRNA levels of TNF-α (B) and IL-6 (C) were evaluated. The relative transcript levels (%) of TNF-α and IL-6 in each group to those in the untreated group (IMQ (-)) are shown. Data are mean ± S.D. (n=4). * P<0.05, ** P<0.01.

Fig. 5. Amelioration of epidermis hyperplasia in psoriasis model rats by NF-κB decoy ODN delivered via IP combined with AT1002 analog pretreatment.

IP administration of NF-κB decoy ODN (50 μg dose/rat) and pretreatment with AT1002 analog (400 μg dose as AT1002) IP were performed as shown in Fig. 3A. At 24 h after IP of NF-κB decoy ODN, the 10-μm frozen skin sections were prepared and stained with HE. Images of skin sections from untreated (A; n=3), IMQ-treated psoriasis model rats (B; n=3), and psoriasis model rats treated with NF-κB decoy IP alone (C; n=3) or combined with AT1002 analog pretreatment (D; n=3). Scale bars = 100 μm. The average epidermis layer thickness of each group of rats was measured

from >20 images of HE-stained skin sections per rat (E). Data are mean ± S.D. (n=3). ** $P<0.01$.

Table 1. Primer sequences for real-time RT-PCR.

Gene	Forward (5' to 3')	Reverse (5' to 3')
TNF-α	CGTAGCAAACCACCAAGCA	CGTAGCAAACCACCAAGCA
IL-6	TCCTACCCCAACTTCCAATGCTC	TTGGATGGTCTTGGTCCTTAGCC
GAPDH	CCCCCAATGTATCCGTTGTG	TAGCCCAGGATGCCCTTTAGT

Fig. 1

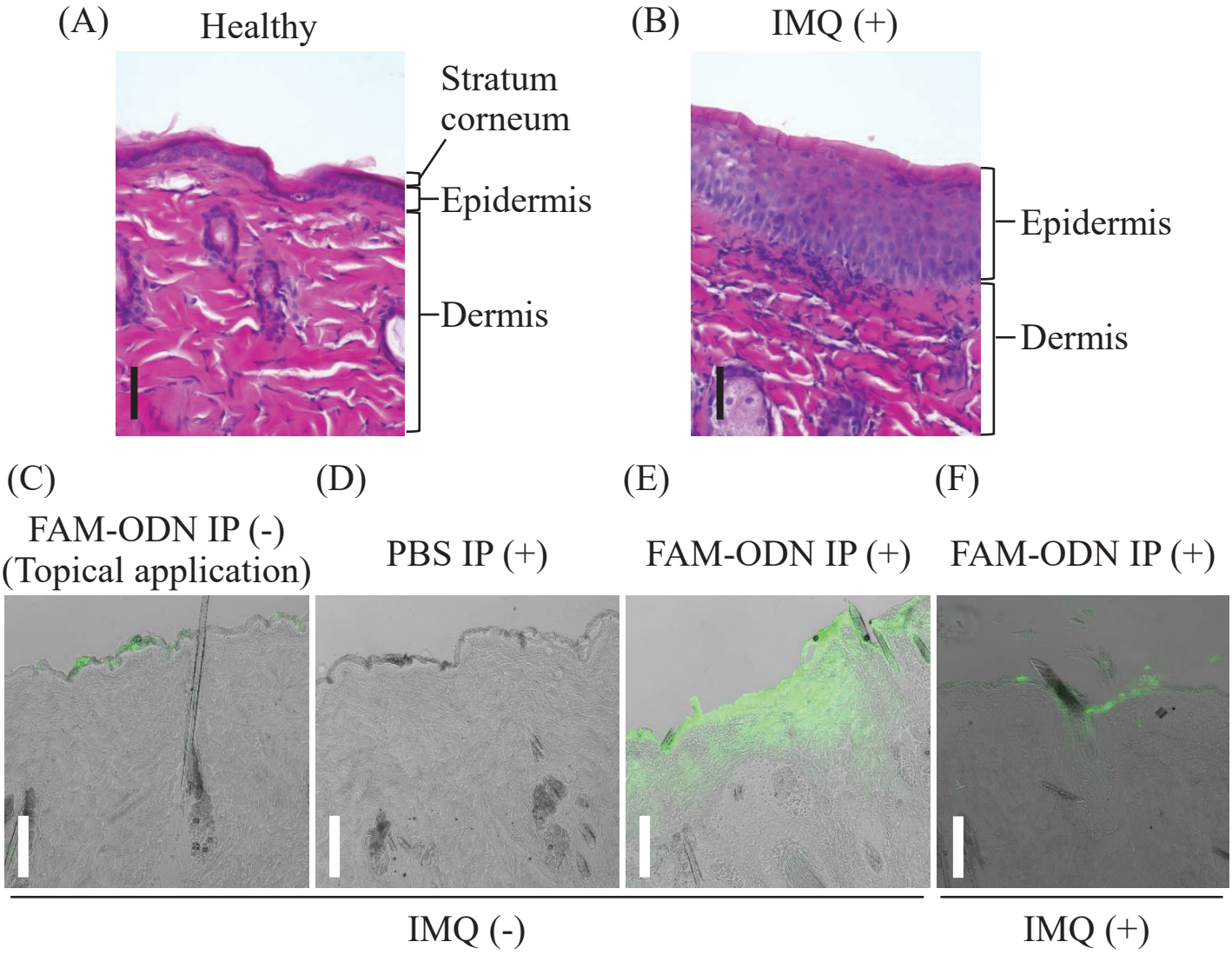
(A)
Healthy
Stratum corneum
Epidermis
Dermis
(B)
IMQ (+)
Epidermis
Dermis
(C)
FAM-ODN IP (-)
(Topical application)
(D)
PBS IP (+)
(E)
FAM-ODN IP (+)
(F)
FAM-ODN IP (+)
IMQ (-)
IMQ (+)

Fig. 2

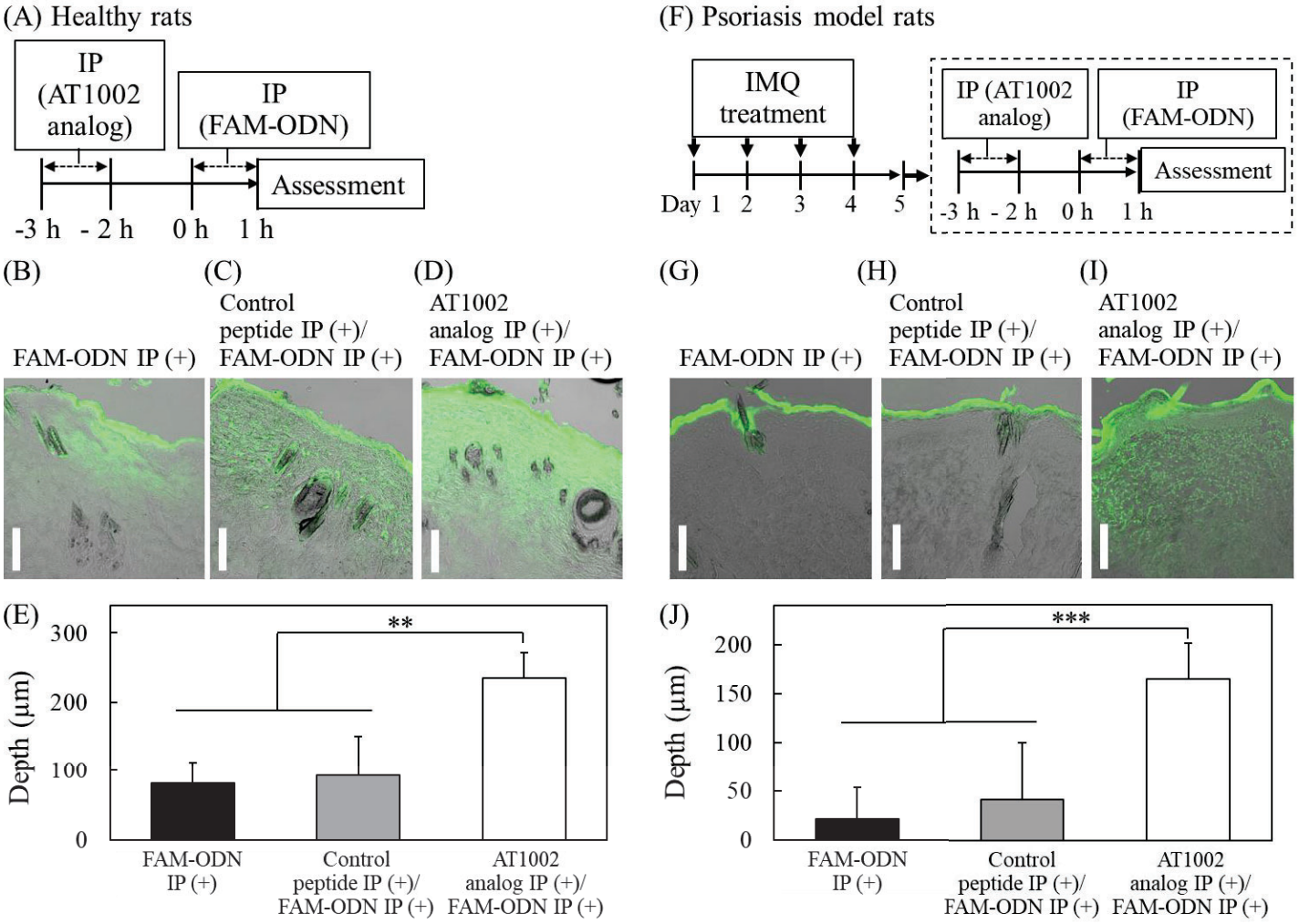
(A) Healthy rats
IP (AT1002 analog)
IP (FAM-ODN)
Assessment
-3 h
- 2 h
0 h
1 h
(F) Psoriasis model rats
IMQ treatment
Day 1
2
3
4
5
IP (AT1002 analog)
IP (FAM-ODN)
Assessment
-3 h
- 2 h
0 h
1 h
(B)
FAM-ODN IP (+)
(C)
Control peptide IP (+)/ FAM-ODN IP (+)
(D)
AT1002 analog IP (+)/ FAM-ODN IP (+)
(G)
FAM-ODN IP (+)
(H)
Control peptide IP (+)/ FAM-ODN IP (+)
(I)
AT1002 analog IP (+)/ FAM-ODN IP (+)
(E)
Depth (μm)
300
200
100
0
**
FAM-ODN IP (+)
Control peptide IP (+)/ FAM-ODN IP (+)
AT1002 analog IP (+)/ FAM-ODN IP (+)
(J)
Depth (μm)
200
150
100
50
0
***
FAM-ODN IP (+)
Control peptide IP (+)/ FAM-ODN IP (+)
AT1002 analog IP (+)/ FAM-ODN IP (+)

Fig. 3

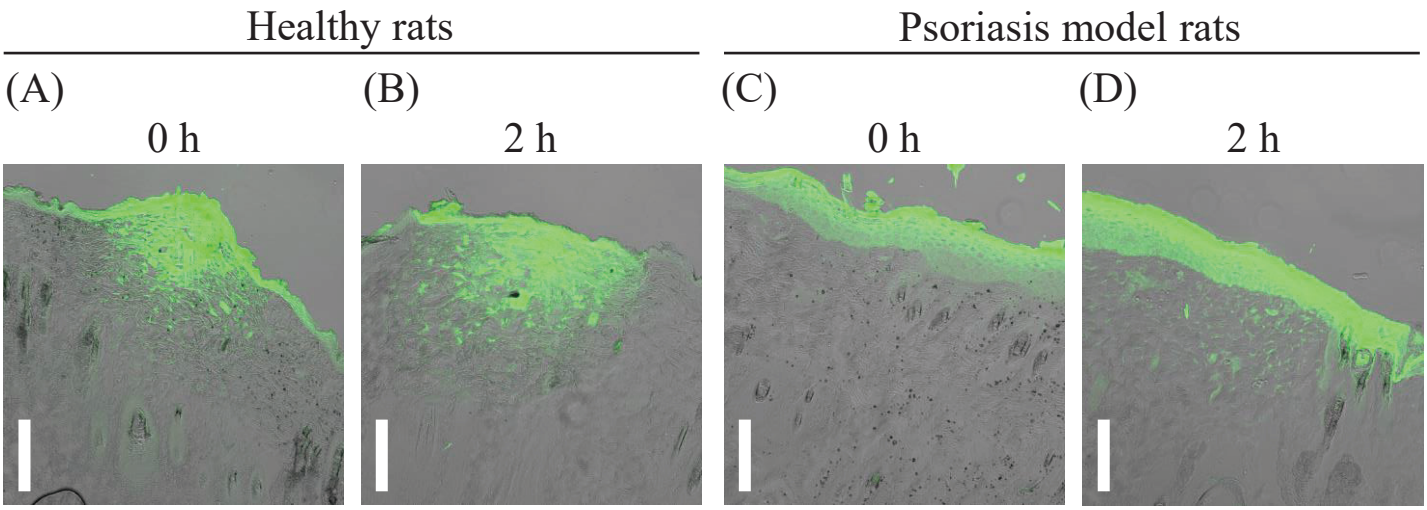

Fig. 4

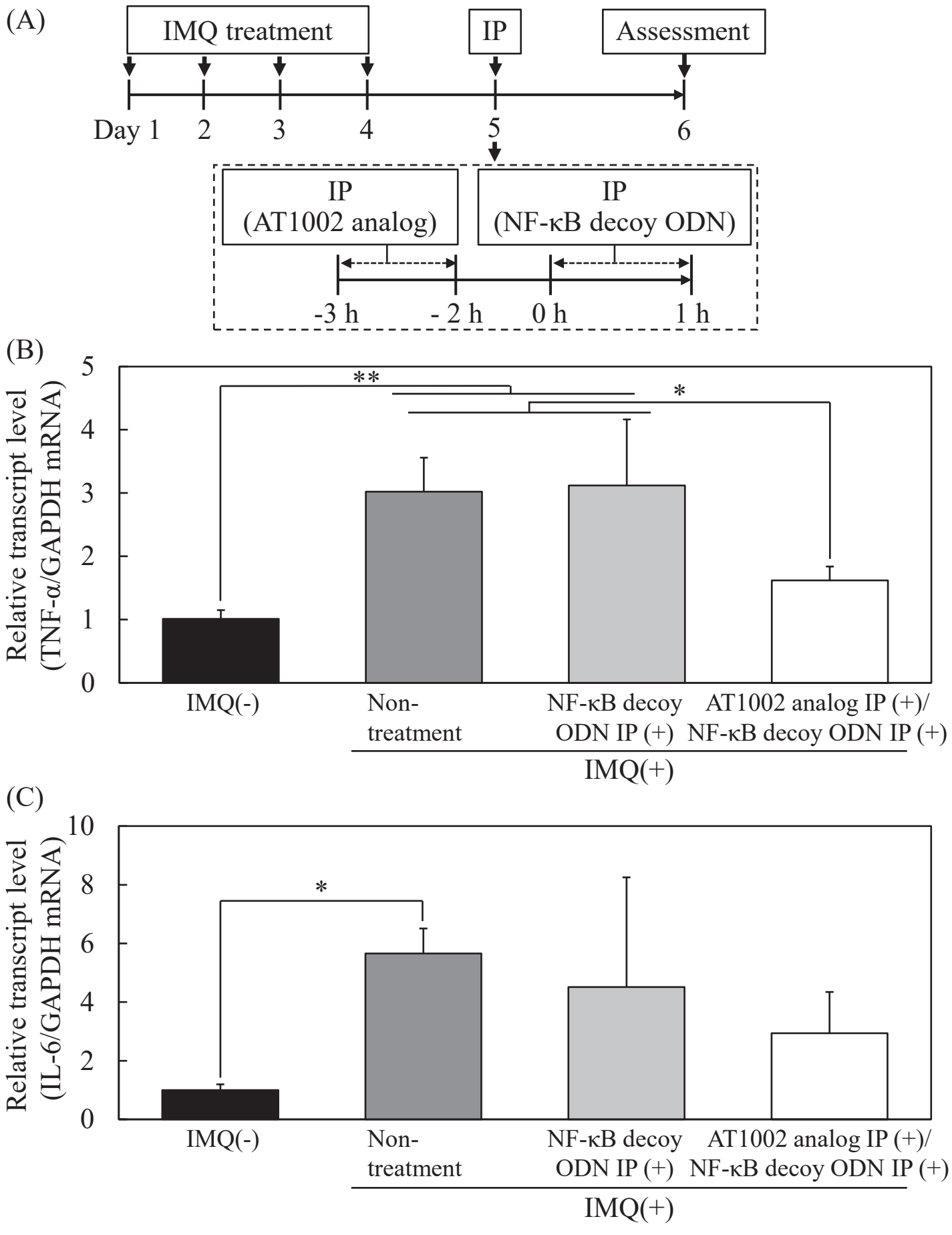
(A)
IMQ treatment
IP
Assessment
Day 1
2
3
4
5
6
IP
(AT1002 analog)
IP
(NF-κB decoy ODN)
-3 h
- 2 h
0 h
1 h
(B)
Relative transcript level
(TNF-α/GAPDH mRNA)
0
1
2
3
4
5
**
*
IMQ(-)
Non-
treatment
NF-κB decoy
ODN IP (+)
AT1002 analog IP (+)/
NF-κB decoy ODN IP (+)
IMQ(+)
(C)
Relative transcript level
(IL-6/GAPDH mRNA)
0
2
4
6
8
10
*
IMQ(-)
Non-
treatment
NF-κB decoy
ODN IP (+)
AT1002 analog IP (+)/
NF-κB decoy ODN IP (+)
IMQ(+)

Fig. 5

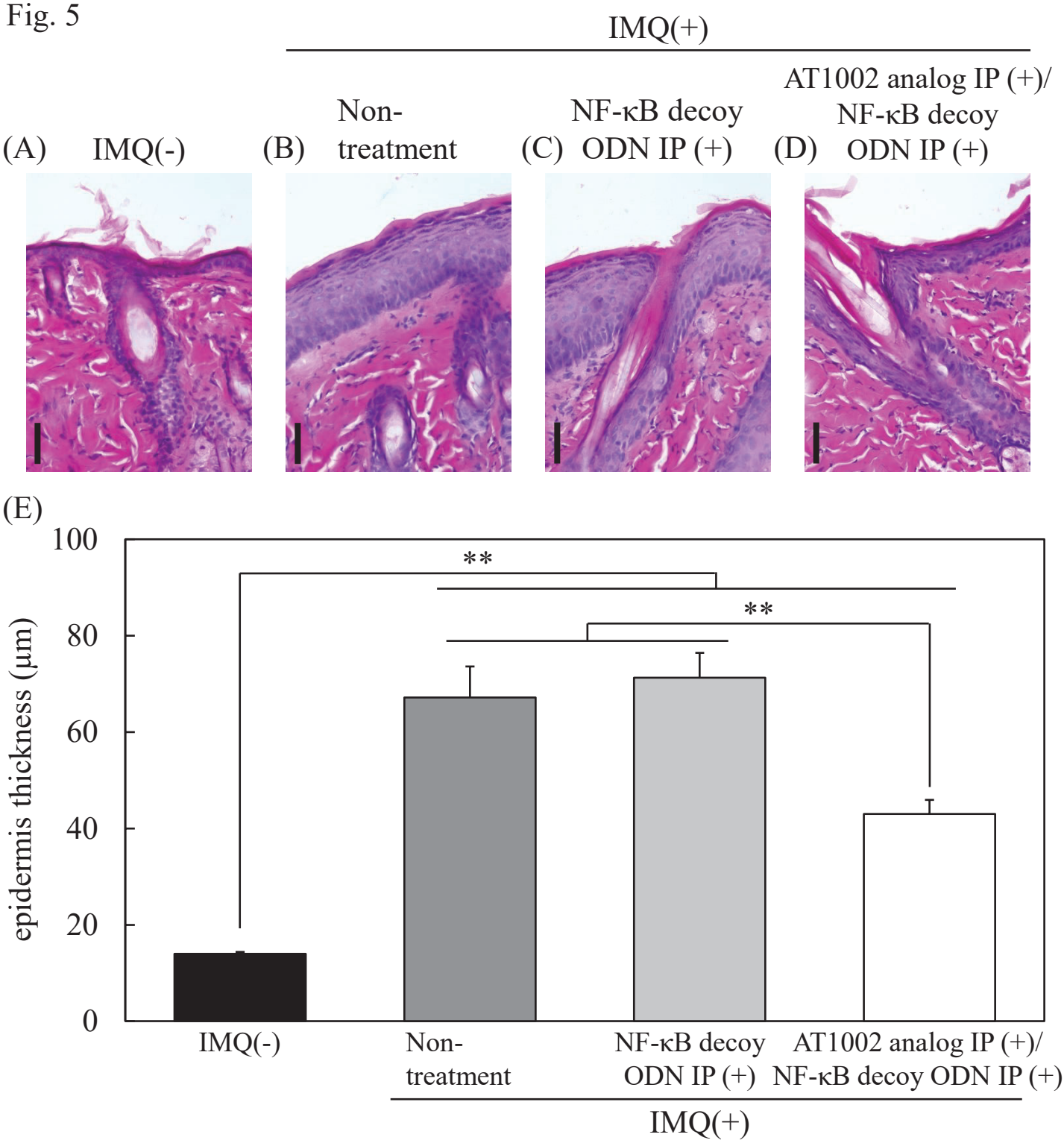
IMQ(+)
(A) IMQ(-)
(B) Non-treatment
(C) NF-κB decoy ODN IP (+)
(D) AT1002 analog IP (+)/ NF-κB decoy ODN IP (+)
(E)
epidermis thickness (μm)
100
80
60
40
20
0
**
**
IMQ(-)
Non-treatment
NF-κB decoy ODN IP (+)
AT1002 analog IP (+)/ NF-κB decoy ODN IP (+)
IMQ(+)